ACERP: Vol. 6, No.1, (Winter 2020) 22-29

Advanced Ceramics Progress

Research Article

Journal Homepage: www.acerp.ir

The Impact of Current Density of Electroplating on Microstructure and Mechanical Properties of Ni-ZrO_2-TiO_2 Composite Coating

T. Ameri Ekhtiarabadi [a], M. Zandrahimi [a *], H. Ebrahimifar [b]

[a] *Department of Metallurgy and Materials Science, Faculty of Engineering, Shahid Bahonar University of Kerman, Kerman, Iran*

[b] *Department of Materials Engineering, Faculty of Mechanical and Materials Engineering, Graduate University of Advanced Technology, Kerman, Iran*

PAPER INFO

Paper history:

Received 15 December 2019
Accepted in revised form 03 February 2020

Keywords:

Composite Coating
TiO_2
ZrO_2
Current Density
Abrasive Resistance

ABSTRACT

Metallic composite coatings with ceramic particles can be used to improve the mechanical and corrosion properties of steel. In the present research, Ni-ZrO_2-TiO_2 composite coating was fabricated on AISI 430 stainless steel through the electrodeposition method. The effect of the current density of electroplating (15, 17, 20, and 23 $mA.cm^{-2}$) was investigated on the microstructure and mechanical behavior of coated steel. Scanning electron microscopy (SEM) and X-ray diffraction (XRD) were used to study the morphology and phases. Micro-hardness was measured by the Wickers method, and wear behavior was evaluated by the pin-on-disk test. The results showed that the deposition of TiO_2 and ZrO_2 ceramic particles in the composite coating increased and then decreased by increasing the applied current density up to 20 $mA.cm^{-2}$. Similar trends were observed for the variations in hardness and wear resistance of the composite coating. According to the results, the use of Ni-ZrO_2-TiO_2 composite coating on AISI 430 stainless steel improved the mechanical properties.

1. INTRODUCTION

Composite coatings are deposited on various steel substrates to improve the properties such as corrosion and wear resistance. Stainless steel is among the most widely used types of steel in various industries, and therefore, a great deal of research has been done on the coating of stainless steel [1,2].

Metal-based composite coatings are fabricated throughout both electroplating and electroless method. Neutral particles (TiO_2, ZrO_2, SiO_2, SiC, Al_2O_3, etc.) that are suspended in an electric bath can be coincidentally deposited during electroplating. The obtained composite coatings will have higher physical and mechanical properties, such as higher wear and corrosion resistance than pure metal coatings [3].

Since in the composite coatings the properties of the matrix and the secondary particles are combined, special properties such as good strength at high temperature, high thermal conductivity, and low thermal expansion coefficient are obtained [4].

In a study by Hong et al., it was reported that factors such as the concentration of particles in the plating bath, the applied current density, and the pH of the plating bath affect the amount of particle deposition in the coating, the crystalline size, and the mechanical properties of the coating considering the microstructure. Wang et al. investigated the effect of cathodic current density on the weight percent of TiO_2 particles when the particle concentration in the electrolyte is 30 $g.L^{-1}$. Their results showed that the weight percent of TiO_2 particles initially increased with increasing cathodic current density until it reached the maximum value as much as 5$A.dm^{-2}$. As the current density increases, the amount of TiO_2 particles decreases [5].

Qu studied the effect of current density on the amount of CeO_2 particles deposited on Ni-CeO_2 composite coatings. Their results showed that the amount of CeO_2 particles decreased as the current density increased [6].

Titanium oxide is one of the most important particles due to the low thermal expansion coefficient, favorable mechanical properties, and excellent chemical stability at all temperatures as reinforcement to nickel-

* Corresponding Author Email: m.zandrahimi@uk.ac.ir (M. Zandrahimi)

phosphorus coatings [7]. Saravanan et al. [8] showed that titania particles have a great impact on the growth process and the phase structure of the nickel-phosphorus coating, which increases the corrosion resistance. They also showed that adding more amounts of alumina would increase the porosity of the coating and reduce the corrosion resistance.

The reactive element and its oxides can greatly reduce the oxidation rate and increase the resistance of the alloy to cracking [9]. This is commonly known as the reactive element effect, and reactive elements are added to the surface by ion implantation or to the surface as oxide when added as metal alloying elements, oxide dispersion [10,11]. Zirconium is the common reactive element used in composite coatings. Studies have shown that coatings with ZrO_2 significantly reduce the oxidation rate of stainless steel and increase the performance of SOFC interconnects [12].

Laszczyńska et al. [13] investigated the effect of ZrO_2 on the characterization of electrodeposited Ni-Mo-ZrO_2 composite coatings. They reported that ZrO_2 oxide modified the structure and adhesion of Ni-Mo coating [13]. In the recent research by Khoran et al. [14], they investigated the addition of TiO_2 oxide on the microstructure and oxidation behavior of Ni-TiO_2 composite coating. Their studies showed that the addition of TiO_2 to nickel coating decreased in grain size and improvement of oxidation behavior [14]. In another study, Saiedpour et al. [15] investigated the effect of ZrO_2 particles on oxidation and electrical behavior of Co coatings electroplated on ferritic stainless steel interconnect. Their results showed that the addition of ZrO_2 to cobalt coating improved the structure and oxidation behavior of the steel [15].

According to previous studies and a survey of the literature, no Ni-ZrO_2-TiO_2 coating has been fabricated on AISI 430 steel substrate so far. The presence of titanium oxide and zirconium oxide is expected to improve the mechanical properties of the coating.

In the present study, Ni-ZrO_2-TiO_2 composite coating was deposited on AISI 430 steel substrate by the electrodeposition method. Then, the effect of applied current density on microstructure and mechanical properties were investigated. Scanning electron microscopy (SEM) and X-ray diffraction (XRD) were used to determine the microstructure. Finally, a pin on the disk test was performed to evaluate the wear behavior of these coatings.

2. EXPERIMENTAL PROCEDURES

In this study, AISI 430 stainless steel with the chemical composition was used that is given in Table 1. Samples with dimensions of 2mm×10mm×10mm were used as the substrate for coating and pure nickel sheet (purity above 99%) with dimensions as much as 20mm ×20 were used as the anode. Pre-plating preparation of the samples was performed according to the ASTM B254 standard by first polishing the steel plates with abrasives 400, 600, 800, 1200, and 2500.

TABLE 1. Chemical composition of AISI 430 stainless steel (wt%)

Element	Concentration (wt. %)
C	0.12
Cr	17.10
Mn	0.92
Si	0.50
P	0.02
S	0.023
Fe	Bal

The samples were placed in an acetone solution for 10 minutes after washing with distilled water. Then, they were washed again with distilled water and finally etched in 10% sulfuric acid solution for 90 seconds and washed with distilled water after extraction. The samples were placed in the coating bath immediately after preparation. The composition of the bath and the electroplating conditions for the Ni-ZrO_2-TiO_2 composite coating are presented in Table 2.

In this operation, the bath components were first weighed by a digital scale (GF-300 model), and then, added to a 100 ml beaker by adding distilled water. ALFA-HS860 magnetic stirrer was used to mix the materials. The PROVA 8000 power supply was used to generate power. The pH of the solution was adjusted using sulfuric acid or sodium hydroxide and the pH meter of model AZ 8686 was used to control it. Samples were plated at Watts bath at current densities as much as 15, 17, 20, and 23 $mA.cm^{-2}$. The samples were washed with distilled water and dried using a dryer after plating. Microscopic analysis of the samples was carried out using a Scanning Electron Microscope Model Cam Scan MV 2300 equipped with EDS analysis. The morphology of the samples was investigated by SEM at a voltage as much as 20KV.

Phases were identified using a Philips X-ray diffraction device with Cu Kα radiation (λ=0.1542 nm). The XRD patterns of the samples were analyzed using X-Pert software.

Two methods were applied to check the wear resistance of the coated samples. In the first method, each sample was weighed before and after the abrasion test by a scale of four decimal places. The wear behavior of Ni-ZrO_2-TiO_2 composite coating was studied by the pin-on-disk wear. The wear test was performed by the pin-on-disk method with a distance of 100 and a disk rotation speed as much as 0.03 $m.s^{-1}$. The mass change of the samples before and after the wear test was measured using a scale

of four decimal places. The friction coefficient results were analyzed using CDT125 software. All wear tests were done based on ASTM G 99-17 and previous studies [8].
Microhardness of the samples was determined using a Shimadzu hardness tester and applied force as much as 50g for 10s.

TABLE 2. Composition and bath conditions for Ni-ZrO_2-TiO_2 composite coating

Coating Mixtures		Electrodeposition Parameters/Materials	
$NiSO_4.6H_2O$	280.00 g/L	Current density	15, 17, 20, 23 $mA.cm^{-2}$
$NiCl_2.6H_2O$	40.00 g/L	pH	3.5
H_3BO_3	40.00 g/L	Plating time	20 min
$CoSO_4.7H_2O$	6 g/L	Plating temperature	50±5 °C
ZrO_2	3, 5, 7, 9 g/L	Cathode	AISI 430 stainless steel
TiO_2	3, 5, 7, 9 g/L	Anode	Nickel plate

3. RESULTS AND DISCUSSION

3.1. Influence of Current Density on Structure

3.1.1. Deposition of ZrO_2 and TiO_2 Particles

Figure 1 shows the impact of current density on the deposition of ZrO_2 and TiO_2 particles in Ni-ZrO_2-TiO_2 composite coating at concentrations of 5 $g.L^{-1}$ ZrO_2 and 7 $g.L^{-1}$ TiO_2, and pH as much as 3.5. As can be seen the deposition is increased by increasing the current density up to 20$mA.cm^{-2}$ due to the increased mobility of the ZrO_2 and TiO_2 particles. The maximum particle deposition amount was obtained at the current density as much as 20 $mA.cm^{-2}$. The electrophoretic force for moving of ZrO_2 and TiO_2 particles toward the cathode is low at low current densities, resulting in lower particle deposition at low densities.
According to the Guglielmi model [11,14], the particle inclusion in metal matrix from an electroplating solution occurs in two consecutive steps of adsorption, including the "loose adsorption" and "strong adsorption of the particles. The first step is a loose physical adsorption of the particles on the cathode with a high degree of coverage and without the discharge of electro-active ions adsorb on the particles. The fractional coverage follows a Langmuir adsorption isotherm. The second step is the strong electrochemical adsorption of the particles caused by the applied electrochemical field, which is accompanied by the discharge of electro-active ions. Both steps take place at the same time all over the cathode surface. If a particle is strongly adsorbed on the cathode, it will be embedded in the growing metal layer by the electrodeposition of free solvated electro-active ions from the plating bath.
As stated by the Guglielmi model, the particle movement increases with increasing current density. This increase in particle movement causes the ZrO_2 and TiO_2 particles to leave the surface before the second stage adsorption is completed and the particle deposition decreases. Particles recede is due to the high activity of ZrO_2 and TiO_2.
This is due to the high activity of the particles of ZrO_2 and TiO_2 [16]. The nickel ions dissolved in the anode are transported faster than the ZrO_2 and TiO_2 particles traveling with mechanical turbulence at densities higher than the optimum current density (20 $mA.cm^{-2}$), which, thus, reduces the particle deposition of ZrO_2 and TiO_2 in the coating. In the coating [17], the increase in current density causes the release of hydrogen on the cathode surface, which forms the hydrogen bubbles. These bubbles prevent the deposition of particles on the cathode surface and reduce the amount of Co absorption [18].

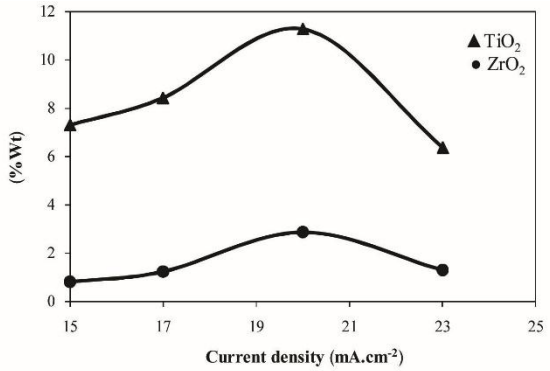

Figure 1. Particle deposition value as a function of current density at concentrations of 5 $g.L^{-1}$ ZrO_2 and 7 $g.L^{-1}$ TiO_2 and pH as much as 3.5

3.1.2. Surface Morphology

Figure 2 shows the effect of current density on the morphology of Ni-ZrO_2-TiO_2 composite coatings. As can be seen the content of ZrO_2 and TiO_2 particles in the coating increases by increasing the current density from 15 to 20 $mA.cm^{-2}$. There is a drop in the deposition of both particles at current densities more than 20 $mA.cm^{-2}$. The decrease in a deposition is due to the release of hydrogen at high current density.
The XRD results of the Ni-ZrO_2-TiO_2 composite coating at different current densities at the concentration as much as 5 $g.L^{-1}$ ZrO_2 and 7 $g.L^{-1}$ TiO_2 in the electrolyte and pH=3.5 are shown in Fig. 3. As can be seen, the available phases are Ni (JCPDS, Card No. 001-1266), ZrO_2 (JCPDS, Card No. 014-0534), and TiO_2 (JCPDS, Card No. 021-1236). However, the observed peaks of Fe

(JCPDS, Card No. 003-1050) are related to the substrate.

It is obvious that the grain size decreases with increasing current density. Figure 2a shows the SEM image of a sample electroplated at a current density as much as 15 $mA.cm^{-2}$. As shown, the coating is not uniform and some agglomeration is observed. At the current density as much as 17 $mA.cm^{-2}$, the irregularity of the coating is less and the coating is more uniform than the obtained value at the current density as much as 15 $mA.cm^{-2}$. The coating obtained at a density as much as 20 $mA.cm^{-2}$ is uniform without cracking and agglomeration. The coating is not uniform at i=23 $mA.cm^{-2}$ and the agglomeration is observed in some places.

Maud software was employed to investigate the effect of current density on phase formations based on the XRD patterns. The amount of precipitated ZrO_2 and TiO_2 was calculated by Maud software. The outputs of the Maud software were consistent with the results of SEM images and XRD analysis. As can be seen the number of ceramic particles ZrO_2 and TiO_2 to the current density as much as 20 $mA.cm^{-2}$ increased by increasing the current density. The SEM images also show that the grain size decreased and the structure was fine by increasing the concentration of ceramic particles ZrO_2 and TiO_2 up to the current density as much as 20 $mA.cm^{-2}$. As the current density increases, the peak intensity of the ZrO_2 and TiO_2 phases increases up to 20 $mA.cm^{-2}$, indicating an increase in the deposition of these particles in the composite coating. This was also observed in other studies [16,17].

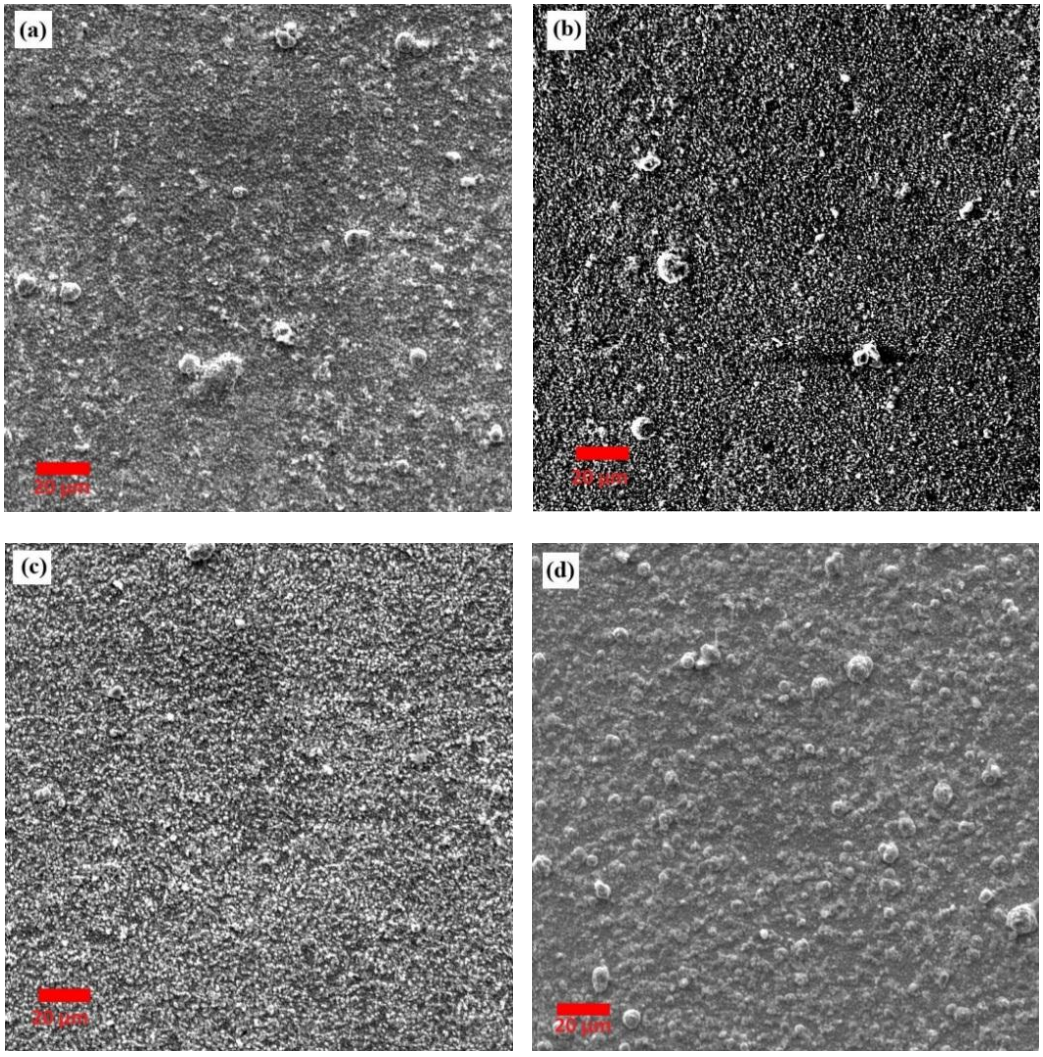

Figure 2. Surface morphology of Ni-ZrO_2-TiO_2 coating deposited under different current densities. a) 15$mA.cm^{-2}$, b) 17$mA.cm^{-2}$, c) 20$mA.cm^{-2}$, and d) 23$mA.cm^{-2}$

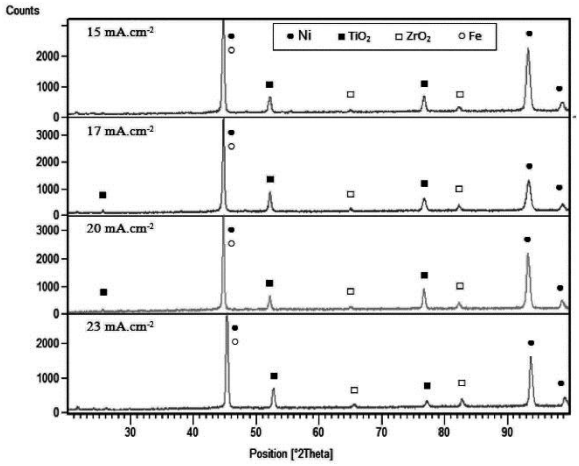

Figure 3. XRD results of Ni-ZrO_2-TiO_2 composite coating at different current densities

3.1.3. Grain Size

The grain size was calculated by the Williamson Hall equation using Equation (1) and Sigma Plot software [17, 18]:

$$\beta \cos\theta = (0.9 \times \lambda)/d + 2 \sin\theta \quad (1)$$

where λ is the x-ray wavelength in angstrom (1.5406 Å), d is the crystallite size, β is the maximum peak width at half the height of the peak, θ is the brag angle corresponding to the peak, and A is a constant (usually one).

Fig. 4 shows the effect of current density on the grain size of Ni-ZrO_2-TiO_2 composite coating at the concentration as much as 5 $g.L^{-1}$ ZrO_2 and 7 $g.L^{-1}$ TiO_2 in the electrolyte and pH=3.5. As can be seen the grain size decreases by increasing current density from 15$mA.cm^{-2}$ to 20 $mA.cm^{-2}$. Increasing the current density above 20 $mA.cm^{-2}$ increases the grain size. The obtained grain size at the current density as much as 20 $mA.cm^{-2}$ is about 17nm.

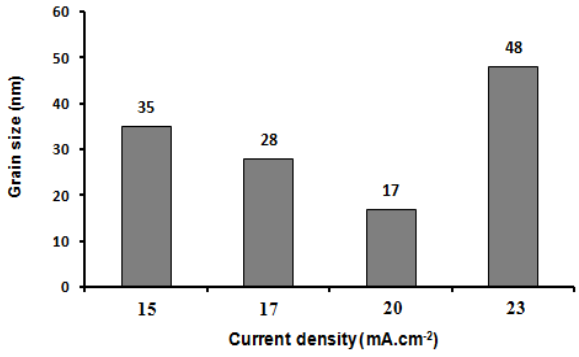

Figure 4. The Influence of current density on the grain size of Ni-ZrO_2-TiO_2 composite coating

According to Equation 2, the nucleation rate increases by increasing current density overvoltage increases and according to equation 3 with increasing overvoltage. The grain size decreases with increasing nucleation rate. Also according to equation 4 the critical radius of nucleation decreases by increasing overvoltage [5,7]:

$$\eta = a + b \log i \quad (2)$$

$$j = K1 \exp[-bs\varepsilon\text{^}2/zekT\eta] \quad (3)$$

$$r = s\varepsilon/ze\eta \quad (4)$$

In Equation (2) η is the overvoltage, a and b are constant, and i is the current density.

In equations (3) and (4), j is the nucleation rate, b is the geometrical factors of the cluster shape, s is the area occupied by an atom, ε is the specific edge energy, z is the ion capacity, e is Electron flux, k_1 is constant and k is Boltzmann constant.

In electrochemistry, overvoltage is the potential difference (voltage) between the determined thermodynamically reduction potential of half-reaction and the potential at which the redox event is experimentally observed [18,19]. The term is directly related to a cell's voltage efficiency. In an electrolytic cell, the existence of overvoltage implies the cell requires more energy than thermodynamically expected to drive a reaction.

In fact, *J* was given by Equation (2) according to the classical theories on electrochemical phase formation and growth, the two dimensional (2D) nucleation rate.

Regarding crystallization theory, crystallization in an electrodeposition process usually involves two steps.

The first step is about the discharge of nickel ions and the generation of nickel atom. There are two scenarios in the second step, (i) the incorporation of nickel atom into the crystal and crystal growth, and (ii) the formation of the new nucleus when the rate of crystal growth may not be sufficient to cater for a generation of atoms. It has been proved that r is a function of the overvoltage in the critical radius of the surface nucleus [19-21].

On the other hand, the number of nucleation sites is increased with increasing particle deposition on the cathode surface, resulting in smaller grain size. The movement of particles and ions increase by increasing the current density up to 23 $mA.cm^{-2}$. Therefore, prior to completing the second step according to Guglielmi's theory, they receded due to the high activity of ZrO_2 and TiO_2 as soon as they deposited. The amount of particles has reduced, the number of nucleation sites has decreased, and the previously formed nuclei have grown and resulted in more coarse grains [10].

3.2. The Impact of Current Density on Mechanical Properties

3.2.1 Microhardness of Coating

Figure 5 shows the microhardness of the coatings as a function of applied current density at concentrations as much as 5 $g.L^{-1}$ ZrO_2 and 7 $g.L^{-1}$ TiO_2, and pH=3.5. As shown, the microhardness increases and reaches its maximum value at 20 $mA.cm^{-2}$ by increasing the applied current density, which is 284.03 Vickers. Increasing the current density above 20 results in a decrease in microhardness. The microhardness reduces to 135.4 Vickers at the current density as much as 23 $mA.cm^{-2}$.

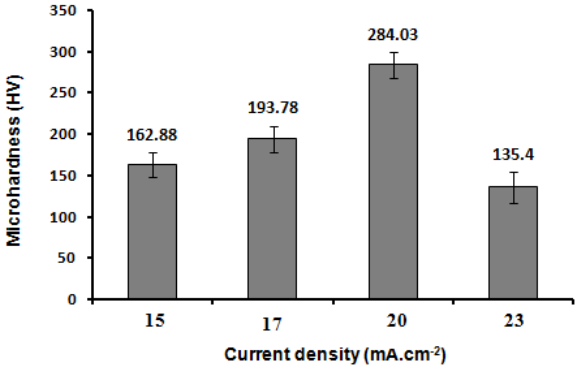

Figure 5. Microhardness changes as a function of current density at concentrations 5 $g.L^{-1}$ ZrO_2 and 7 $g.L^{-1}$ TiO_2, and pH=3.5

One of the mechanisms that increase the microhardness of the composite is the Orowan mechanism. In the Orowan equation (relation 5), λ is the distance between scattered particles, G is shear stress, and b is burgers vector. The smaller the distance between the scattered particles, the greater the shear strength. As a result, an increase in dispersed particles decreases the value of λ, which increases σ. This increase in stress increases the amount of microhardness (Equation 5).

$$\sigma = 2Gb/\lambda \quad (5)$$

High current density levels are not suitable for deposition and coating properties [20].

3.2.2. Coefficient of Friction

Figure 6 shows the effect of the concentration of ZrO_2 and TiO_2 particles on the kinetic friction coefficient of Ni-ZrO_2-TiO_2 composite coating. μk is the kinetic friction coefficient that opposes the range of relative motion. The kinetic friction coefficient decreases with increasing the current density up to 20 $mA.cm^{-2}$. This decrease is due to the high-deposited amounts of ZrO_2 and TiO_2 particles on the Ni-ZrO_2-TiO_2 composite coating at a current density as much as 20 $mA.cm^{-2}$. At the mentioned density, the highest amount of ZrO_2 and TiO_2 particles are obtained by the uniform distribution. As a result, the coating is fine-grained and has the highest microhardness. The presence of particles in the coating reduces the contact area between the pin and the coating surface, and reduces the coefficient of friction. The coefficient of friction increases by increasing current density to 23 $mA.cm^{-2}$ due to the decrease in particle deposition [21].

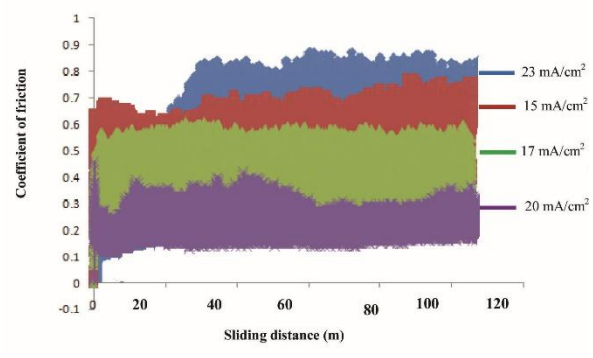

Figure 6. Influence of current density on kinetic friction coefficient at 100m

3.2.3. Wear Resistance

Figure 7 shows the weight loss of Ni-ZrO_2-TiO_2 composite coating based on current density. The weight of the samples decreases by increasing the current density up to 20 $mA.cm^{-2}$. The lowest weight loss at the current density as much as 20 $mA.cm^{-2}$ is 0.2 mg. This procedure follows Archard's Law (Equation 6) [22]:

$$W = k(P_n\ L)/H \quad (6)$$

Where W is the sample weight loss after wear test, k is coefficient of wear, Pn is normal pressure in wear test, L is the distance traveled in wear test, and H is the hardness of the sample.

According to Archard's interface, the weight loss of the sample under abrasion is directly related to the sample pressure and slips distance, which is inversely related to the hardness of the sample under abrasion. Thus, the weight loss of the sample decreased with increasing the microhardness.

Another reason is the Hall-Patch mechanism, which is based on grain size. The highest microhardness was observed at the current density as much as 20 $mA.cm^{-2}$. The microhardness and wear resistance decreases with increasing the distance from each side as the grain size increases and the deposition rate of ZrO_2 and TiO_2 particles decreases.

Another reason is that according to the Orowan equation, the particles in the coating prevent the plastic deformation of the coating by preventing the

deformation of the particles. This is due to the dispersion of the particles in the coating, and consequently, increasing the microhardness and wear resistance [23].

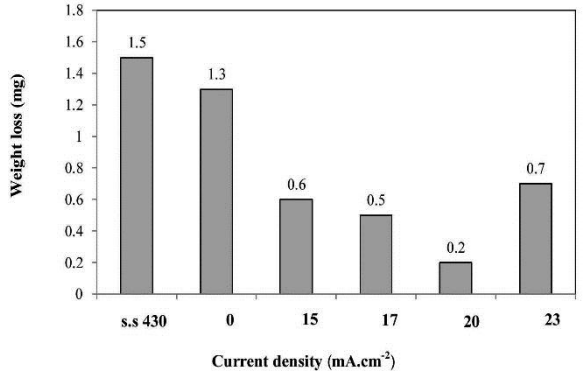

Figure 7. The Influence of current density on the weight loss of Ni-ZrO_2-TiO_2 composite coating

4. CONCLUSION

The Ni-ZrO_2-TiO_2 composite coating was fabricated on AISI 430 stainless steel at different current densities as much as 15, 17, 20, and 23 mA.cm^{-2}, and the following results were obtained:

1. Their deposition amount was increased by increasing the current density up to 20 mA.cm^{-2} due to the increased mobility of the ZrO_2 and TiO_2 particles. The maximum particle deposition value was obtained at the current density as much as 20 mA.cm^{-2}.
2. The number of nucleation sites increased with increasing particle deposition on the cathode surface and the grain size was decreased as the number of nucleation sites increased.
3. The lowest kinetic friction coefficient was obtained for the coated samples at the current density as much as 20 mA.cm^{-2}. This was due to the highest deposition of ZrO_2 and TiO_2 particles on the Ni-ZrO_2-TiO_2 composite coating at a current density as much as 20 mA.cm^{-2}.
4. The wear resistance was increased by increasing the current density of coating up to 20 mA.cm^{-2}. Wear resistance was increased by increasing the microhardness due to the increase in ceramic particles of ZrO_2 and TiO_2.

5. ACKNOWLEDGEMENTS

The authors would like to acknowledge the financial supports given by the University of Shahid Bahonar of Kerman.

REFERENCES

1. Sheu, H. H., Huang, P. C., Tsai, L. C., Hou, K. H., "Effects of plating parameters on the Ni-P-Al_2O_3 composite coatings prepared by pulse and direct current plating", ***Surface and Coatings Technology***, Vol. 235, (2013), 529-535.
2. Alizadeh, M., Mirak, M., Salahinejad, E., Ghafferi, M., Amini, R., Roosta, A., "Structural characterization of electro-codeposited Ni-Al_2O_3- SiC nanocomposite coatings", ***Journal and Alloys and Compounds***, Vol. 611, (2014), 161-166.
3. Hag, I. U., Akhtar, K., Khan, T. I., Shah, A. A., "Electrodeposition of Ni-Fe_2O_3 nanocomposite coating on steel", ***Surface and Coating Technology***, Vol. 235, (2013), 691-698.
4. Szczygieł, B., Kołodziej, M., "Composite Ni/Al_2O_3 coatings and Their corrosion resistance", ***Electrochemical Acta***,Vol. 50, No. 20, (2005), 4188-4195.
5. Wang, Y., Shu, X., Gao, W., Shakoor, R. A., Kahraman, R., Yan, P., Lu, W., Yan, B., "Microstructure and properties of Ni-Co-TiO_2 composite coatings fabricated by electroplating", ***International Journal of Modern Physics B***, Vol. 29, No. 10n11, (2015), 1540008.
6. Qu, N.S., Qian, W.H., Hu, X.Y., Zhu, Z.W., "Fabrication of Ni-CeO_2 Nanocomposite Coatings Synthesised via a Modified Sediment Co-Deposition Process", ***International Journal of Electrochemical Science***, Vol. 8, No. 9, (2013), 11564-11577.
7. Wang, Y., Cao, D., Gao, W., Qiao, Y., Jin, Y., Cheng, G., Gao, W., Zhi, Z., "Microstructure and properties of sol-enhanced Co-P-TiO_2 nano-composite coatings", ***Journal of Alloys and Compounds***, Vol. 792, No. 5, (2019), 617-625.
8. Saravanan, I., Elayaperumal, A., Devaraju, A., Karthikeyan, M., Raji, A., "Wear behaviour of electroless Ni-P and Ni-P-TiO_2 composite coatings on En8 steel", ***Materials Today Proceedings***, Vol. 22, No. 3, (2020), 1135-1139.
9. Jiang, Y., Xu, Y., Feng, G., Yao, H., "High-frequency pulse electrodeposition and characterization of Ni–Co/ZrO_2 nanocomposite coatings", ***Journal of Materials Science: Materials in Electronics***, Vol. 27, No. 8, (2016), 8169-8176.
10. Li, S., Ju, P., Zhang, Y., Zhang, X., Zhao, X., Tang, Y., Zuo, Y., Pu, L., "Effect of Bath ZrO_2 Concentration on the Properties of Ni-Co/ZrO_2 Coatings Obtained by Electrodeposition", ***International Journal of Electrochemical Science***, Vol. 13, No. 8, (2018), 7688-7695.
11. Li, B., Zhang, W., Li, D., "Synthesis and properties of a novel Ni–Co and Ni–Co/ZrO_2 composite coating by DC electrodeposition", ***Journal of Alloys and Compounds***, Vol. 821, (2020), 153258.
12. Li, B., Mei, T., Du, S., Zhang, W., "Synthesis of Ni–Fe and Ni–Fe/ZrO_2 composite coating and evaluation of its structural and corrosion resistance", ***Materials Chemistry and Physics***, Vol. 243, (2020), 122595.
13. Laszczyńska, A., Winiarski, J., Szczygieł, B., Szczygieł, I. "Electrodeposition and characterization of Ni-Mo-ZrO_2 composite coatings", ***Applied Surface Science***, Vol. 369, (2016), 224-231.
14. Khoran, E., Zandrahimi, M., Ebrahimifar, H., "Microstructure and Oxidation Behavior of Ni–TiO_2 Composite Coating at High Temperature", ***Oxidation of Metals***, Vol. 91, No (1-2), (2019), 177–189.
15. Saeidpour, F., Zandrahimi, M., Ebrahimifar, H., "Effect of ZrO_2 particles on oxidation and electrical behavior of Co coatings electroplated on ferritic stainless steel interconnect", ***Corrosion Science***, Vol. 153, (2019), 200-212.
16. Wang, S. C., Wei, W. C. J., "Kinetics of electroplating process of nano-sized ceramic particle/Ni composite", ***Materials Chemistry and Physics***, Vol. 78, No. 3, (2003), 574-580.
17. Ranjith, B., Kalaignan, G. P., "Ni–Co–TiO_2 nanocomposite coating prepared by pulse and pulse reversal methods using acetate bath", ***Applied Surface Science***, Vol. 257, No. 1., (2010), 42- 47.

18. Abed, F. A., "Deposition of Ni-CO/TiO_2 Nanocomposite Coating by Electroplating", ***International Journal of Advanced Research***, Vol. 3, No. 1, (5015), 241-246.
19. Qu, N. S., Zhu, D., Chan, K. C., Lei, W. N., "Pulse electrodeposition of nanocrystalline nickel using ultra narrow pulse width and high peak current density", ***Surface and Coatings Technology***, Vol. 168, No. (2-3), (2003), 123-128.
20. Jeyaraj, S., Arulshri, K. P., Sivasakthivel, P. S., "Effects of Process Parameters on Microhardness of Electrodeposited Ni-Al Composite Coating Using Taguchi Method", ***Portugaliae Electrochimica Acta***, Vol. 33, No. 5, (2015), 249-264.
21. Sun, X. J., Li, J. G., "Friction and Wear Properties of Electrodeposited Nickel-Titania Nanocomposite Coatings", ***Tribology Letters***, Vol. 28, No. 3, (2007), 223-228.
22. Zmitrowicz, A., "Wear patterns and laws of wear- A review" ***Journal of Theoretical and Applied Mechanics***, Vol. 44, No. 2, (2006), 219-253.
23. Rupert, T. J., Schuh, C. A., "Sliding wear of nanocrystalline Ni-W: Structural evolution and the apparent breakdown of Archard scaling", ***Acta Materialia***, Vol. 58, No. 12, (2010), 4137-4148.